A novel dye-modified metal-organic framework as bifunctional fluorescent probe for visual sensing for styrene and temperature

Jie Yang [1], Chaojun Ren [2], Min Liu [1], Wenwei Li [1], Daojiang Gao [1], Hongda Li [3], and Zhanglei Ning [1,*]

[1] College of Chemistry and Materials Science, Sichuan Normal University, Chengdu 610068, China
[2] Beijing Aerospace Propulsion Institute, Beijing, 100076, China
[3] Liuzhou Key Laboratory for New Energy Vehicle Power Lithium Battery, School of Electronic Engineering, Guangxi University of Science and Technology, Liuzhou 545006, China
* Correspondence: Corresponding author.
E-mail address:Yangjie_deyouxiang@163.com (Yang, J.); rcj_ustb@163.com (Ren, C.-J); liumin200009@163.com (Liu, M.); liwenwen202202@163.com (Li, W.-W); daojiangao@sicnu.edu.cn (Gao, D.-J.); hdli@gxust.edu.cn (Li, H.-D.); zlning@sicnu.edu.cn (Ning, Z.-L.)

Abstract: A novel fluorescent probe (C460@Tb-MOFs) was designed and synthesized through encapsulating the fluorescent dye 7-diethylamino-4-methyl coumarin into terbium-based metal-organic framework by a simple ultrasonic impregnation method. It is impressive that this dye-modified metal-organic framework can specifically detect styrene and temperature upon luminescence quenching. The sensing platform of this material exhibit great selectivity, fast response and good cyclability toward styrene detection. It is worth mentioning that the sensing process undergoes a distinct color change from blue to colourless, providing conditions for accurate visual detection of styrene liquid and gas. The significant fluorescence quenching mechanism of styrene toward C460@Tb-MOFs is explored in detail. Moreover, the dye-modified metal-organic framework can also achieve temperature sensing from 298 to 498 K with high relative sensitivity at 498 K. The preparation of functionalized MOFs composites by fluorescent dyes provides an effective strategy for the construction of sensors for multifunctional applications.

Keywords: MOFs; fluorescent probe; dye; styrene; temperature sensing

1. Introduction

Metal organic frameworks (MOFs) materials have attracted much attention due to their porosity, large specific surface area, versatility and tunable functionality[1, 2]. As typical porous materials, MOFs can be used as a unique perform for stabilizing and limiting functional substances, which allow the development of diverse MOFs composites and their application in different fields[3-5]. In particular, the encapsulating of fluorescent dye into the pore spaces of MOFs greatly reduces aggregation-induced quenching effect of dyes, which did not change the original structure of MOFs[6]. In addition, the dye still has good photochemical stability due to the protection of the MOFs framework. The dye-modified metal-organic framework possess dual fluorescent groups from the MOFs and dyes, extending the range of applications to cell staining, fluorescence immunization and fluorescent probes[7-10].

Volatile organic compounds (VOCs) are generally defined as organic compounds with a saturated vapour pressure above 133.32 Pa at room temperature and a boiling point below 250°C at an atmospheric pressure of 100 kPa[11, 12]. When VOCs are present in the environment at certain concentrations, they can have a significant impact on human health. Irritating odours can cause fatigue and headaches, nausea and vomiting in the short term, and even cause adverse effects such as coma and convulsions. In addition, long-term exposure to VOCs can have even more detrimental effects on the human body, including damage to the kidneys, liver, central nervous system and even cancer[13, 14].

 doi:10.20944/preprints202306.0219.v1

Styrene, a typical component of VOCs, is used in the synthetic resin, pharmaceutical, dye, pesticide, and mineral processing industries[15-17]. Styrene is classified as a Group 2B carcinogen by the World Health Organization's International Agency for Research on Cancer and can be absorbed by the body through the respiratory tract and skin[18]. Several methods have been reported for the detection of VOCs, mainly gas chromatography, thermal desorption mass spectrometry, Fourier transform infrared spectrometry, atomic emission spectrometry and semiconductor electrochemistry[19-22]. However, the above detection methods have some inevitable problems, such as complex operational processes, long detection times and high technical requirements, all of which can limit widespread detection. Therefore, developing a simple, time-saving and low-cost way to the accurate measurement of styrene is of great importance.

Temperature is a fundamental physical parameter of great importance in human life, scientific research and industry. Temperature is not only a key factor in the growth of plants and animals, but also plays a crucial role in the fields of optics, electrochemistry and biomedicine[23, 24]. Early thermometers were contact thermometers, which often measured temperature by changes in volume, potential and conductance, but were less suitable in certain special environments (liquids, cells or inside the body, etc.). Luminescent thermometers have received much attention in the field of non-contact optical temperature measurement due to their simplicity, high sensitivity and accuracy, and the temperature dependence of fluorescence is used as an indicator of temperature sensing. In recent years, many composite MOFs materials with fast response and high relative sensitivity have been explored and developed for use as luminescent thermometers[25, 26].

In this work, a dye C460-modified C460@Tb-MOFs composite was synthesized. It can be applied as a fluorescent probe for visual recognition of styrene liquid and gas, exhibiting high sensitivity and fast response rate. The quenching mechanism of styrene by the C460@Tb-MOFs composite is also explored. The portable C460@Tb-MOFs luminescent silica gel plate was prepared to obtain a more visual inspection of styrene detection. Moreover, the C460@Tb-MOFs composite can be used as a fluorescence probe for temperature sensing from 298 to 498 K. Overall, this work provides a simple strategy for multifunctional MOFs and opens the way for versatile applications in MOFs composites.

2. Experimental section

2.1. Reagents and instruments

All chemical reagents and solvents used in this work are commercially available analytical grade and are used directly without further purification. Terbium nitrate hexahydrate ($Tb(NO_3)_3.6H_2O$), mucic acid (MA) and potassium hydroxide (KOH) were obtained from Aladdin Chemistry Co., Ltd (Shang hai, China). Benzene, toluene, ethylbenzene, o-xylene, formaldehyde, acetaldehyde, propionaldehyde, butyl acetate and styrene were purchased from Chengdu Kelong Chemical Co., Ltd (Chengdu, China).

2.2. Synthesis of Tb-MOFs and C460@Tb-MOFs

The Tb-MOFs sample is synthesized by a fast and facile method at room temperature condition[27, 28]. The C460@Tb-MOFs composites were synthesized by simple ultrasonic impregnation method. First, the Tb-MOFs were immersed in an ethanolic solution of 60 mM C460, the mixture was shaken uniformly by sonication and kept in equilibrium for 30 min, and then immersed at room temperature for 24 h. Finally, the resulting precipitate was collected and dried at 60 °C for 24 h to obtain a yellow-green solid, which was finely ground and then sealed in a dry environment for storage.

2.3. Fluorescence sensing of detection styrene liquid

C460@Tb-MOFs were dissolved in ethanol solution and sonicated to form a homogeneous suspension. A series of 10^{-3} M solutions of VOCs (benzene, toluene, ethylbenzene,

 doi:10.20944/preprints202306.0219.v1

o-xylene, formaldehyde, acetaldehyde, propionaldehyde, butyl acetate and styrene) were then added to the suspension and tested for fluorescence.

2.4. Fluorescence sensing of detection styrene gas

Sodium carboxymethyl cellulose and silica gel were dissolved to obtain a uniform mixture of solution, and then coated on a glass slide and left to dry to obtain a matrix silica gel plate. The C460@Tb-MOFs was evenly dispersed in the PVA solution, and then it was evenly dropped on the silica gel plate. The C460@Tb-MOFs luminous silica gel plate was prepared by constant temperature drying, and it was used to detect VOCs gas.

3. Results and discussion

3.1. Characterization of C460@Tb-MOFs fluorescent probe

Fig. 1a shows the XRD of the reported Tb-MOFs, the synthetic Tb-MOFs, the dye C460 and the C460@Tb-MOFs, respectively. The XRD of the synthesized Tb-MOFs is in a pure phase, which is consistent with diffraction peak positions of the reported Tb-MOFs. In addition, the diffraction peaks of C460@Tb-MOFs with C460 functionalized modification are in the same position as Tb-MOFs and the crystalline structure is not disrupted[29]. However, the characteristic peak of C460 was not evident, probably due to the low loading of C460 in the pores or the surface of the MOFs. The EDX of Tb-MOFs and C460@Tb-MOFs are shown in Fig. S1. The Tb-MOFs contain three elements: C, O and Tb, while the C460@Tb-MOFs contain four elements: C, O, N and Tb, with the same chemical composition as the elemental composition of the target sample. The IR spectra of Tb-MOFs and C460@Tb-MOFs as shown in Fig. S2a. The broad band at 3306 cm^{-1} for Tb-MOFs is the -OH vibrational peak of the water molecule and the strong peak at 3426 cm^{-1} for C460@Tb-MOFs is probably the O-H and N-H stretching vibrations. N_2 adsorption tests on Tb-MOFs and C460@Tb-MOFs are shown in Fig. 1b, the specific surface area and pore volume of Tb-MOFs are 18.4238 m^2/g and 0.0406 cm^3/g, respectively, and that of C460@Tb-MOFs are 6.8437 m^2/g and 0.0256 cm^3/g, respectively, which are reduced by 62.9% and 36.9% compared with Tb-MOFs, indicating that the dye C460 has been introduced into the Tb-MOFs channel or surface. The zeta potentials of C460, Tb-MOFs and C460@Tb-MOFs are shown in Fig. 1c. It can be seen from Fig. 1d that all the surface potentials are negative and the absolute zeta potential value of C460@Tb-MOFs increases to 38.5 mV. The results show that there is an electrostatic attraction (H-H or N-H interaction) between C460 and Tb-MOFs, which promotes the emission of C460 in C460@Tb-MOFs through host-guest energy transfer, and that the system is more stable with a high absolute value of zeta potential for C460@Tb-MOFs[30]. Thermal stability and pyrolysis properties are one of the important properties of the materials, the thermogravimetric curves of Tb-MOFs and C460@Tb-MOFs are shown in Fig. S2b, both Tb-MOFs and C460@Tb-MOFs have three main stages of weight loss, and in the high temperature range of 400 ~ 600 °C, the weight loss rate of C460@Tb-MOFs (14.4%) is smaller than that of Tb- MOFs (24.6%)[31]. The pyrolysis curves of Tb-MOFs and C460@Tb-MOFs are shown in Fig. S2c, the difference between the first thermal cracking temperature of the two samples was not significant, and by comparing the second thermal cracking temperature of C460@Tb-MOFs increased by 31.8 °C, which indicates that C460@Tb-MOFs has good thermal stability and high temperature resistance to pyrolysis. The morphological characteristics of the Tb-MOFs and C460@Tb-MOFs are shown in Fig. S3. All the samples show a large number of small spheres of 3-5 μm in diameter (Fig. S3a, S3c), indicating that the introduction of C460 had no major effect on the microstructure of Tb-MOFs (also confirmed by XRD). Compared with Tb-MOFs, the SEM image of C460@Tb-MOFs displayed rough surface (Fig. S3b, S3d), which may be cause by dye C460 adhered to surface of MOFs. In elemental mapping, four elements O, C, Tb and N (derived from dye C460) were evenly distributed in C460@Tb-MOFs composite (Fig. S4), further indicating the successfully synthesis of C460@Tb-MOFs.

Preprints (www.preprints.org) | NOT PEER-REVIEWED | Posted: 2 June 2023 doi:10.20944/preprints202306.0219.v1

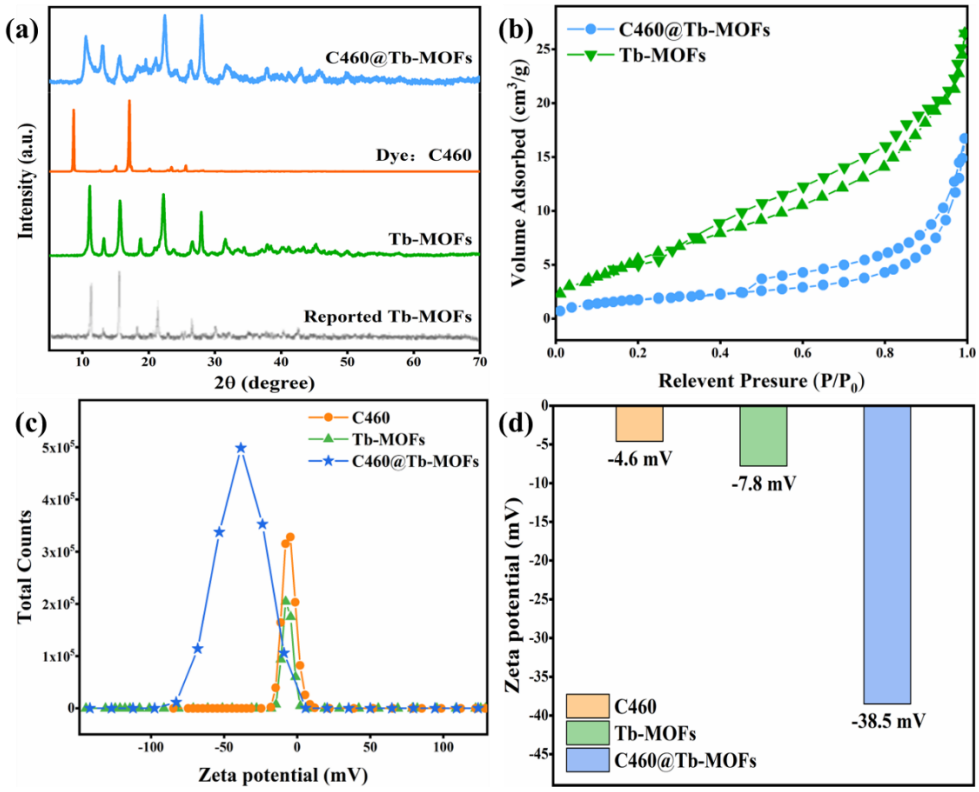

Figure 1. (a) XRD patterns of the reported Tb-MOFs, the synthetic crystalline Tb-MOFs, dye C460 and C460@Tb-MOFs samples; (b) The N_2 adsorption isotherms of Tb-MOFs and C460@Tb-MOFs after heat-treatment; (c) Zeta potential plots of C460, Tb-MOFs and C460@Tb-MOFs; (d) Histograms of zeta potential values of C460, Tb-MOFs and C460@Tb-MOFs.

In order to accurately determine the content of dye C460 in C460@Tb-MOFs, the luminescence intensity of different concentrations of C460 in ethanol was measured. It can be seen that the intensity of materials gradually enhanced as the concentration of C460 increased (Fig. S5a), and the linearly fitted concentration and luminescence intensity is shown in Fig. S5b. The resulting relationship equation is: $I = 1.2180\times10^{8}\ C + 43.6873$ (where I is the luminous intensity; C is the concentration of dye C460). The emission spectra of the actual loading of dye C460 in C460@Tb-MOFs are shown in Fig. S6a ~ d, and the actual loading of C460 in different concentrations of C460@Tb-MOFs are calculated by bringing into equation: (a) 1×10^{-3}M, 0.004%; (b) 1×10^{-2}M, 0.034%; (c) 6×10^{-2}M, 0.49%; (d) 1×10^{-1}M, 0.67%. The luminescence intensity of C460@Tb-MOFs can be modulated by changes in dye concentration. Given that C460@Tb-MOFs are used as ratio-metric fluorescent probes, a sample with a C460 concentration of 6×10^{-2} M and I_{545}/I_{450} of 2.0, with actual loading of 0.49% (Fig. S6c) was selected for subsequent application studies. The emission spectra of C460@Tb-MOFs at different excitation wavelengths are shown in Fig. S7a. A change in excitation wavelength leads to a change in the characteristic emission ratio of Tb^{3+}/C460, 225 nm was chosen as the excitation wavelength for the sample with the best luminescence and emission intensity ratio. The fluorescence emission spectra of C460@Tb-MOFs after immersion in stable solutions at different pH values (pH=3.0~9.0) for 48 h are shown in Fig. S7b, indicating that the samples have good fluorescence stability, laying the foundation for the subsequent practical application of this material. The excitation and emission spectra of Tb-MOFs and C460 are shown in Fig. S8a and b, the excitation and emission spectra of C460@Tb-MOFs are shown in Fig. S8c and d. As shown in Fig. S8c, the characteristic peak was used as the monitoring wavelength with peaks at 225 nm and 368 nm, and 225 nm was chosen as the excitation wavelength in conjunction with Fig. S7a. As shown in Fig. S8d, when C460@Tb-MOFs were excited at 225 nm, double emission peaks appeared at 450 nm and 545 nm[32, 33]. The samples were yellow-green in daylight and

Preprints (www.preprints.org) | NOT PEER-REVIEWED | Posted: 2 June 2023 doi:10.20944/preprints202306.0219.v1

the chromaticity coordinates were (0.175, 0.207) between C460 and Tb^{3+}, indicating that C460@Tb-MOFs have been successfully prepared and are consistent with the blue-green double emission characteristics of C460/Tb^{3+}. The C460 emission peak showed a slight red shift (from 445 nm to 450 nm), which may be due to the enhanced molecular interactions caused by the loading of C460 on the Tb-MOFs.

3.2. C460@Tb-MOFs for real-time detection of styrene liquid and styrene gas

To investigate the ability of C460@Tb-MOFs as fluorescent probe for the detection of volatile organic compounds (VOCs), a series of VOCs solutions (propionaldehyde, formaldehyde, acetaldehyde, benzene, toluene, butyl acetate, ethylbenzene, o-xylene and styrene) were added to C460@Tb-MOFs to obtain a mixture and tested for fluorescence response. As shown in Fig. 2a, the C460@Tb-MOFs have different fluorescence responses to different VOCs liquids.The styrene in the VOCs liquid causes a significant decrease in the intensity of the C460 characteristic peak, and the characteristic emission of Tb^{3+} is almost completely quenched by styrene, indicating that C460@Tb-MOFs has excellent detection selectivity for styrene. Fig. 2b shows the results of the sample testing VOCs liquid under UV light (254 nm), where the fluorescent colour of styrene is significantly quenched and can be directly distinguished by the naked eye. The fluorescence quenching rate of C460@Tb-MOFs for different VOCs solutions are shown in Fig. S9a. The fluorescence quenching rate for other VOCs were below 80% at 450 nm, while the maximum quenching rate for styrene exceeded 80% (85.7%). The quenching rate for styrene was as high as 99.1% at 545 nm as shown in Fig. S9b, which was almost completely quenched. In summary, the C460@Tb-MOFs utilized the double emission feature to selectively detect styrene in VOCs solutions. One of the characteristics of an excellent fluorescent probe is the high selectivity that can be achieved even against complex backgrounds. Anti-interference tests were carried out for styrene as shown in Fig. S10. The fluorescence was almost completely quenched by the addition of styrene, which is consistent with the detection of styrene. This result demonstrates the excellent anti-interference capability of the fluorescent probe.

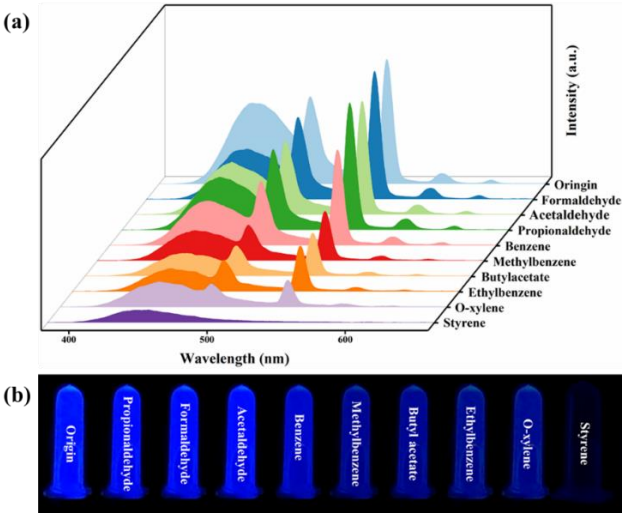

Figure 2. (a) Emission spectra of C460@Tb-MOFs dispersed in different VOCs liquids; (b) Photographs of C460@Tb-MOFs immersed in different VOCs liquids under 254 nm UV dark box irradiation.

The detection sensitivity of C460@Tb-MOFs for styrene liquids is shown in Fig. 3a. The bimodal intensity gradually decreased as the concentration of styrene increased. Fitting the concentration and intensity ratio (I_{545}/I_{450}) as shown in Fig. 3b, there was a good linear relationship for styrene identification in the range of 10^{-5} ~ 10^{-2} M: I_{545}/I_{450} = -0.006 [M] + 1.958 (R^2=0.9973), indicating that C460@Tb-MOFs can be used as a fluorescent probe for the quantitative detection of styrene liquids[34]. The rapid dropwise addition of

Preprints (www.preprints.org) | NOT PEER-REVIEWED | Posted: 2 June 2023 doi:10.20944/preprints202306.0219.v1

styrene liquid to a cuvette of C460@Tb-MOFs suspension for real-time sensing monitoring is shown in Fig. S11a. Within less than 5 s of adding styrene liquid, the bimodal intensity immediately dropped to almost total quenching and remained relatively stable in subsequent quenching, indicating a rapid and time-stable response of C460@Tb-MOFs to detect styrene liquid. Fig. S11b shows the time dependence of I_{545}/I_{450}, visually reflecting the significant detection effect after 5 s of styrene addition and the relative stability in 5~600 s. These results indicate that the C460@Tb-MOFs have a rapid response to styrene detection, showing more advantageous for practical applications.

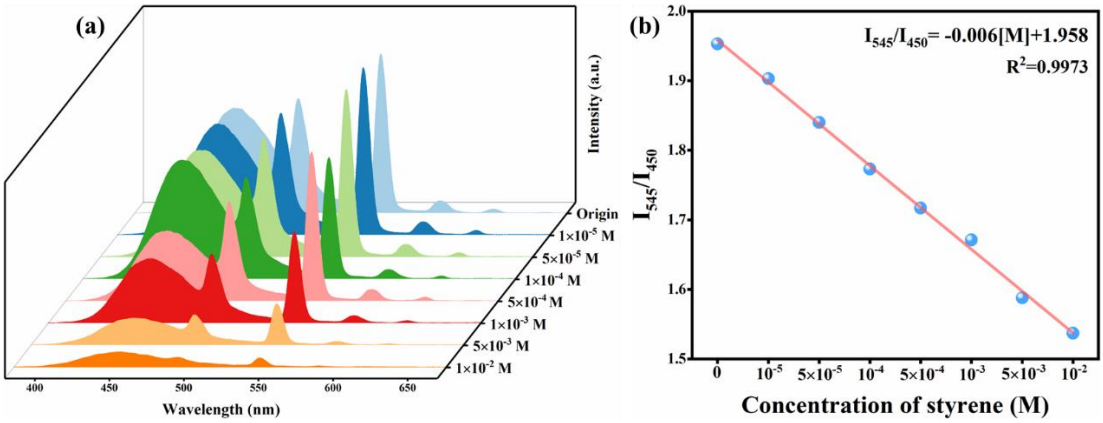

Figure 3. (a) Emission spectra after the addition of different styrene concentrations; (b) Linear plot of styrene concentration against I_{545}/I_{450}.

Given the extremely volatile nature of VOCs, the possibility of C460@Tb-MOFs being used as a fluorescent probe for styrene gas continues to be explored. Portable C460@Tb-MOFs luminescent silica gel plates were prepared to test VOCs gases as shown in Fig. 4a. The detection of different VOCs gases varied, but the most significant quenching effect was for styrene (I_{545}). The luminescent silica gel plate kept in the VOCs gases atmosphere and photographed under the UV dark box (254 nm) are shown in Fig. 4b. The luminescent silica gel plates exhibit superb quenching effect of the luminescent silica gel plate on styrene gas, showing excellent selectivity and visual sensing for styrene gas.

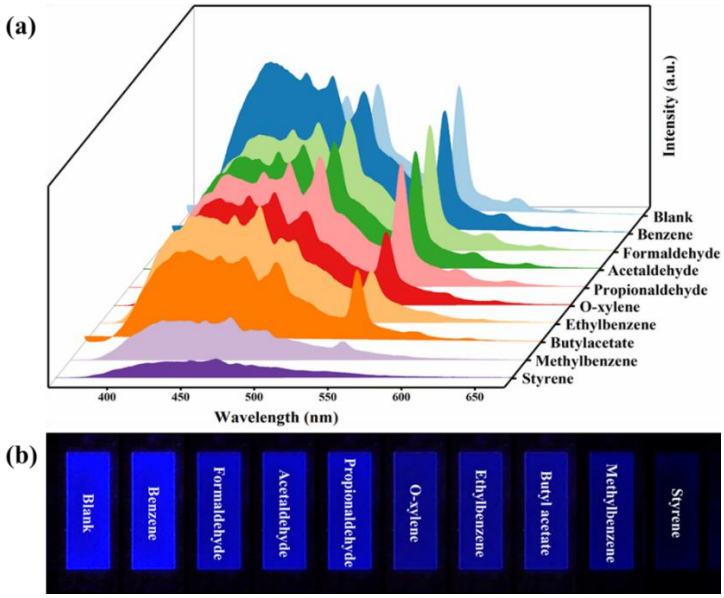

Figure 4. (a) Emission spectra of C460@Tb-MOFs in different VOCs vapor atmospheres; (b) The photographs of C460@Tb-MOFs (after being kept in various VOCs vapor atmospheres for a period of times) under 254 nm UV light irradiation.

Preprints (www.preprints.org) | NOT PEER-REVIEWED | Posted: 2 June 2023 doi:10.20944/preprints202306.0219.v1

The fluorescence quenching rates of C460@Tb-MOFs luminescent silica gel plates for different VOCs gases at 450 nm and 545 nm are shown in Fig. S12a and b. The identification of different VOCs gases differed, but the quenching rate for styrene gas was over 80% (87.5% for I_{450} and 95.0% for I_{545}), therefore C460@Tb-MOFs luminescent silica gel plate can be used as specific detectors for the gas styrene. The results of the temporal response of the C460@Tb-MOFs luminescent silica gel plate to styrene gas detection is shown in Fig. S13a. The intensity of I_{545} decreased significantly within 10 s and was almost completely quenched after 1 min, while the intensity of I_{450} decreased by about 1/3 within 10 s and decreased significantly and remained relatively stable after 1 min. The relative intensity ratio versus time is shown in Fig. S13b. It can be found that intensity ratio changed significant within 10 s of detection, indicating that this C460@Tb-MOFs luminescent silica gel plate is capable of rapid detection of styrene gas. Moreover, the cycling performance of the C460@Tb-MOFs luminescent silica gel plate for styrene gas detection was investigated, and the styrene gas was dried and treated before the next detection. As shown in Fig. S14, the relative fluorescence intensity ratio remained at the initial value for five cycles. The C460@Tb-MOFs luminescent silica gel plate has good cycling performance for styrene gas detection and is expected to be widely used in practical environments due to its outstanding advantages such as portability and cyclability.

3.3. C460@Tb-MOFs sensing mechanism for styrene

The mechanism of fluorescence quench can be attributed to the following: structural disintegration of the material; interaction with rare earth ions; and interaction with ligands. The possible fluorescence quench mechanisms for the detection of styrene are therefore investigated. The XRD of C460@Tb-MOFs after detection of styrene was first tested as shown in Fig. 5a, and the diffraction peak position did not change comparing C460@Tb-MOFs, thus ruling out fluorescence quenching due to structural disintegration of the material.

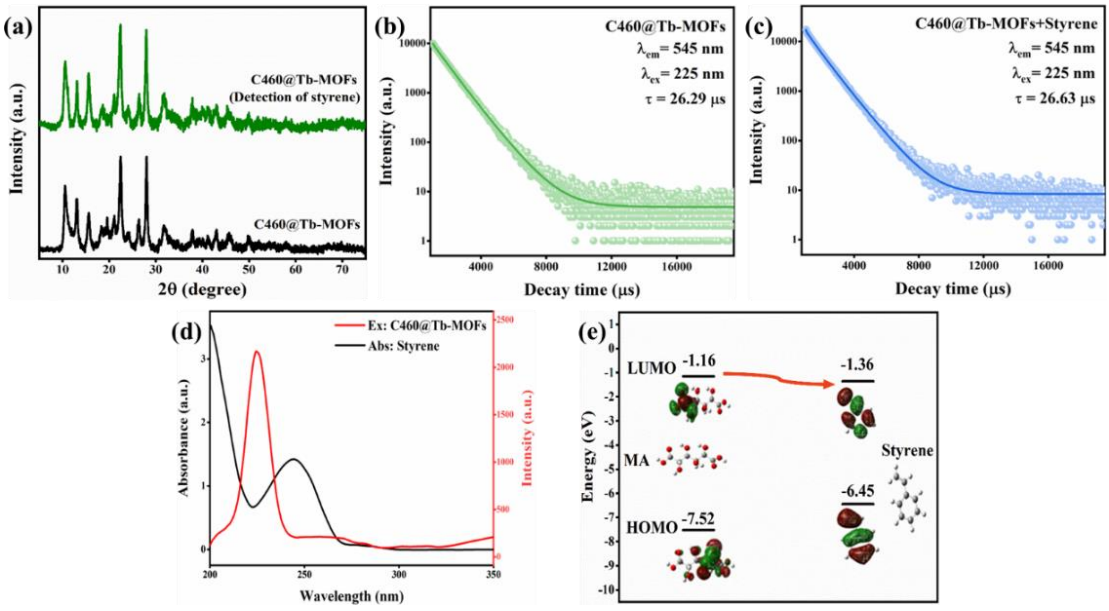

Figure 5. (a) XRD patterns of C460@Tb-MOFs and C460@Tb-MOFs after detection of styrene; (b) and (c) Fluorescence lifetime of C460@Tb-MOFs before and after detection of styrene; (d) Excitation spectra of C460@Tb-MOFs and UV absorption spectra of styrene; (e) The calculated LOMO and HUMO energy levels of ligand mucic acid (MA) and styrene.

The fluorescence quenching mechanism can also be verified by the fluorescence decay lifetime, and the fluorescence lifetime at 545 nm, with the maximum quenching rate, was selected for exploration. As shown in Fig. 5b and c, the fluorescence lifetimes of

 doi:10.20944/preprints202306.0219.v1

C460@Tb-MOFs did not change significantly before and after detection of styrene (before: 26.29 μs; after: 26.63 μs), which is a static quenching process. Since the styrene molecule has no functional groups coordinated to Tb^{3+}, so it is likely that the interaction is with the ligand. Exploring the possible quenching mechanism further, the excitation spectra of C460@Tb-MOFs and the UV absorption spectra of styrene are shown in Fig. 5d. The apparent overlap in the shortwave region leads to fluorescence resonance energy transfer, where the ligand energy is transferred to and absorbed by styrene, reducing the Tb^{3+} "antenna effect" and fluorescence quenching is consistent with a FRET mechanism. The LOMO and HUMO energy levels of the ligand (MA) and styrene molecules were calculated by density functional theory as shown in Fig. 5e. The LUMO energy level of the acceptor styrene (-1.36 eV) is lower than that of the donor MA (-1.16 eV), while the LUMO-HOMO band gap value of styrene (5.09 eV) is lower than that of MA (6.36 eV), so MA as a donor can transfer energy to the acceptor styrene, leading to fluorescence quenching of C460@Tb-MOFs, which is also consistent with the above fluorescence measurements. This suggests that the detection of styrene fluorescence quenching is attributed to a PET mechanism. In summary, the mechanism of styrene detection by fluorescent probes of C460@Tb-MOFs is mainly fluorescence resonance energy transfer (FRET) and photo-induced electron transfer (PET) between styrene and C460@Tb-MOFs.

3.4. C460@Tb-MOFs for temperature sensing

In view of the outstanding fluorescence properties of C460@Tb-MOFs, other properties of this material were investigated. C460@Tb-MOFs were used as fluorescent probes for temperature sensing as shown in Fig. 6a. Fluorescence properties were tested in 298~498 K, with increasing temperature, the characteristic peak of C460@Tb-MOFs was gradually decreasing with good temperature dependence. Fig. 6b shows that the fluorescence intensity of C460 and Tb^{3+} decreases regularly with increasing temperature in 298~498 K. The relationship between C460@Tb-MOFs and temperature was further explored and the results of a linear fit of temperature versus I_{545}/I_{450} are shown in Fig. 6c. From the graph, there is a functional relationship between temperature and I_{545}/I_{450} with the fitted function equation $\lg(I_{545}/I_{450}) = -0.0017x+1.45$ with a linear correlation coefficient (R^2) of 0.9935, indicating that the composite can be act as a ratio-metric fluorescent temperature probe in 298~498 K. In addition, differences in temperature performance of fluorescent temperature probes can be compared by the relative sensitivity (S_r), which is defined as self-calibrating luminescence thermometry as shown below:

$$S_r = \left| \frac{\partial Y / \partial T}{Y} \right|$$

In the above equation S_r is the relative sensitivity, Y is the $\lg(I_{545}/I_{450})$ intensity ratio and T is the temperature. The calculated relative sensitivity results in 298~498 K are shown in Fig. 6d, where S_r for C460@Tb-MOFs exhibits regular variation, with S_r at 498 K still maintaining 0.55% K^{-1}, which is better than S_r at high temperatures for other materials (Table 1).

Preprints (www.preprints.org) | NOT PEER-REVIEWED | Posted: 2 June 2023 doi:10.20944/preprints202306.0219.v1

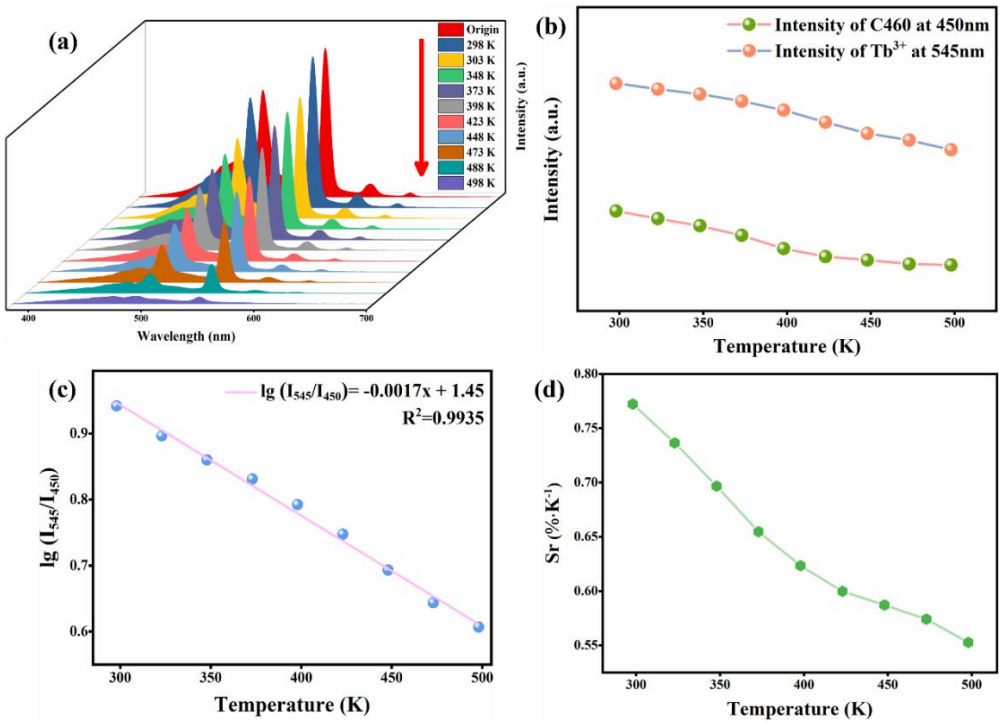

Figure 6. (a) Emission spectra of C460@Tb-MOFs in different temperature ranges (298~498 K); (b) Trends of fluorescence intensity with temperature at 450 nm and 545 nm for C460@Tb-MOFs, respectively; (c) Linear fits of temperature (298~498 K) related to the intensity ratio of I_{545}/I_{450}; (d) Relative sensitivity of C460@ Tb-MOFs with temperature-dependent relative sensitivity.

Table 1. Comparison of relative sensitivity of luminescent MOFs in different temperature ranges.

MOFs	Temperature range (K)	S_r (% K^{-1})	Max temperature (K)	Ref
Rh101@UiO-67	293~333	1.19	333	[35]
$Tb_{0.99}Eu_{0.01}(BDC)_{1.5}(H_2O)_2$	300~320	0.37	320	[36]
Cdots&RB@ZIF-8	293~353	0.74	353	[24]
Eu@Uio-(bpydc)	293~353	0.31	353	[25]
Dycpia	298~473	0.42	473	[26]
$[Eu_{0.7}Tb_{0.3}(cam)(Himdc)_2(H_2O)_2]_3$	100~450	0.079	450	[37]
$[Tb_{0.99}Eu_{0.01}(hfa)_3(dpbp)]_n$	200~300	0.52	300	[38]
$Tb_{0.9}Eu_{0.1}L$	40~300	0.11	300	[39]
$[(Tb_{0.9382}Eu_{0.0616})(bpcd)_2(NO_3)_2]Cl$	25~200	0.34	200	[40]
$Tb_{0.92}Eu_{0.08}$-HPIDC-OX	303~473	0.36	473	[23]
C460@Tb-MOFs	298~498	0.55	498	this work

4. Conclusions

In summary, we proposed a facile strategy to obtain a novel blue-green dual-emitting functionalized C460@Tb-MOFs composite by simple introducing dye into Tb-MOFs. Experimental results show that the developed C460@Tb-MOFs can be used as an outstanding fluorescent probe for the specific detection of styrene liquids with great selectivity, fast response and high sensitivity. In addition, the home-made luminescent silica gel plates can directly discriminate styrene gas by the naked eye with excellent cycling performance. The quenching mechanism can be a combination of FRET and PET rules. Moreover, C460@Tb-MOFs can also respond well as a temperature probe to achieve temperature sensing at 298~498 K with high relative sensitivity at high temperatures. To the best of our knowledge, the study gives an example to realize styrene detection and

 doi:10.20944/preprints202306.0219.v1

temperature sensing simultaneously for the first time, which successfully extends the application of metal-organic framework in the field of fluorescence recognition.

Acknowledgments This work was financially supported by the Project of Science & Technology Department of Sichuan Province (No. 2021YFG0277) and Open Foundation of Key Laboratory of Special Wastewater Treatment of Sichuan Province Higher Education System (SWWT2020-2).

Reference

1. Li, Q.; Chen, H.; You, S.; Lin, Z.; Chen, Z.; Huang, F.; Qiu, B. Colorimetric and fluorescent dual-modality sensing platform based on UiO-66 for fluorion detection. *Microchem. J.* **2023,** *186*, 108318.
2. Liu, M.; Ren, X.; Meng, X.; Li, H. Metal-organic frameworks-based fluorescent nanocomposites for bioimaging in living cells and in vivo. *Chin. J. Chem.* **2021,** *39*, 473-487.
3. Cai, H.; Lu, W.; Yang, C.; Zhang, M.; Li, M.; Che, C.-M.; Li, D. Tandem Förster resonance energy transfer induced luminescent ratiometric thermometry in Dye-encapsulated biological metal–organic frameworks. *Advanced Optical Materials.* **2019,** *7*, 1801149.
4. Ruan, B.; Yang, J.; Zhang, Y.-J.; Ma, N.; Shi, D.; Jiang, T.; Tsai, F.-C. UiO-66 derivate as a fluorescent probe for Fe^{3+} detection. *Talanta.* **2020,** *218*, 121207.
5. Fan, M.; Yan, J.; Cui, Q.; Shang, R.; Zuo, Q.; Gong, L.; Zhang, W. Synthesis and Peroxide Activation Mechanism of Bimetallic MOF for Water Contaminant Degradation: A Review. *Molecules*. **2023**, *28*, 3622.
6. Fan, Y.; Jiang, X.; Che, J.; Li, M.; Zhang, X.; Gao, D.; Bi, J.; Ning, Z. A Ratiometric Fluorescent Sensor Based on Dye/Tb (III) Functionalized UiO-66 for Highly Sensitive Detection of TDGA. *Molecules*. **2022**, *27*,6543.
7. Liu, J.; Yue, X.; Wang, Z.; Zhang, X.; Xu, Y. Coumarin 7 functionalized europium-based metal–organic-framework luminescent composites for dual-mode optical thermometry. *J. Mater. Chem. C.* **2020,** *8*, 13328-13335.
8. Liu, L.; Lu, X.-Y.; Zhang, M.-L.; Ren, Y.-X.; Wang, J.-J.; Yang, X.-G. 2D MOF nanosheets as an artificial light-harvesting system with enhanced photoelectric switching performance. *Inorg Chem Front.* **2022,** *9, (11),* 2676-2682.
9. Wang, X.; Wang, X.; Han, Y.; Li, H.; Kang, Q.; Wang, P.; Zhou, F. Immunoassay for cardiac troponin I with fluorescent signal amplification by hydrolyzed coumarin released from a metal–organic framework. *ACS Applied Energy Materials.* **2019,** *2, (11),* 7170-7177.
10. Feng, D.; Zhang, T.; Zhong, T.; Zhang, C.; Tian, Y.; Wang, G. Coumarin-embedded MOF UiO-66 as a selective and sensitive fluorescent sensor for the recognition and detection of Fe^{3+} ions. *J. Mater. Chem. C.* **2021,** *9, (47),* 16978-16984.
11. Shen, Y.; Tissot, A.; Serre, C. Recent progress on MOF-based optical sensors for VOC sensing. *Chemical Science.* **2022,** *13, (47),* 13978-14007.
12. Li, X.; Zhang, L.; Yang, Z.; Wang, P.; Yan, Y.; Ran, J. Adsorption materials for volatile organic compounds (VOCs) and the key factors for VOCs adsorption process: a review. *Sep. Purif. Technol.* **2020,** *235*, 116213.
13. Tung, T. T.; Tran, M. T.; Feller, J.-F.; Castro, M.; Van Ngo, T.; Hassan, K.; Nine, M. J.; Losic, D. Graphene and metal organic frameworks (MOFs) hybridization for tunable chemoresistive sensors for detection of volatile organic compounds (VOCs) biomarkers. *Carbon.* **2020,** *159*, 333-344.
14. Joshi, M.; Nair, S. Hplc analysis of trigonella foenum-graecum seeds to assess phytoestrogens. *Indian Journal of Occupational and Environmental Medicine.* **2008,** *12, (2)*, 61-64.
15. Kim, S.-I.; Kim, A.-R.; Bae, H. J.; Kim, S.-Y.; Ravi, S.; Kim, K. C.; Bae, Y.-S. Cu(I)-incorporation strategy for developing styrene selective adsorbents. *Chem. Eng. J.* **2021,** *425*, 130601.
16. Yang, F.; Ma, J.; Zhu, Q.; Ma, Z.; Wang, J. Aggregation-induced luminescence based UiO-66: highly selective fast-response styrene detection. *ACS Appl. Mater. Interfaces.* **2022,** *14, (19)*, 22510-22520.
17. Kim, S.-I.; Kim, A.-R.; Kim, S.-Y.; Lee, J.-Y.; Bae, Y.-S. High styrene/ethylbenzene selectivity in a metal-organic framework with coordinatively unsaturated cobalt(II) sites. *Sep. Purif. Technol.* **2020,** *242*, 116758.
18. Sarigiannis, D. A.; Karakitsios, S. P.; Gotti, A.; Liakos, I. L.; Katsoyiannis, A. Exposure to major volatile organic compounds and carbonyls in european indoor environments and associated health risk. *Environ. Int.* **2011,** *37, (4)*, 743-765.
19. Ras, M. R.; Borrull, F.; Marcé, R. M. Sampling and preconcentration techniques for determination of volatile organic compounds in air samples. *TrAC, Trends Anal. Chem.* **2009,** *28, (3)*, 347-361.
20. Zhang, Y.; Zhao, J.; Du, T.; Zhu, Z.; Zhang, J.; Liu, Q. A gas sensor array for the simultaneous detection of multiple VOCs. *Sci. Rep.* **2017,** *7, (1)*, 1960.
21. Park, J.; Tabata, H. Gas sensor array using a hybrid structure based on zeolite and oxide semiconductors for multiple bio-gas detection. *ACS Omega.* **2021,** *6, (33)*, 21284-21293.
22. Qin, P.; Okur, S.; Li, C.; Chandresh, A.; Mutruc, D.; Hecht, S.; Heinke, L. A photoprogrammable electronic nose with switchable selectivity for VOCs using MOF films. *Chem. Sci.* **2021,** *12, (47)*, 15700-15709.
23. Yang, Y.; Huang, H.; Wang, Y.; Qiu, F.; Feng, Y.; Song, X.; Tang, X.; Zhang, G.; Liu, W. A family of mixed-lanthanide metal–organic framework thermometers in a wide temperature range. *Dalton Trans.* **2018,** *47, (38)*, 13384-13390.
24. Ding, Y.; Lu, Y.; Yu, K.; Wang, S.; Zhao, D.; Chen, B. MOF-nanocomposite mixed-matrix membrane for dual-luminescence ratiometric temperature sensing. *Advanced Optical Materials.* **2021,** *9, (19),* 2100945.

 doi:10.20944/preprints202306.0219.v1

25. Zhou, Y.; Yan, B. Ratiometric detection of temperature using responsive dual-emissive MOF hybrids. *J. Mater. Chem. C.* **2015,** *3, (36)*, 9353-9358.
26. Xia, T.; Cui, Y.; Yang, Y.; Qian, G. A luminescent ratiometric thermometer based on thermally coupled levels of a Dy-MOF. *J. Mater. Chem. C.* **2017,** *5, (21)*, 5044-5047.
27. Wong, K.-L.; Law, G.-L.; Yang, Y.-Y.; Wong, W.-T. A highly porous luminescent terbium–organic framework for reversible anion sensing. *Advanced Materials.* **2006,** *18, (8)*, 1051-1054.
28. Yang, J.; Che, J.; Jiang, X.; Fan, Y.; Gao, D.; Bi, J.; Ning, Z. A novel turn-on fluorescence probe based on Cu(II) functionalized metal– organic frameworks for visual detection of uric acid. *Molecules.* **2022,** *27, (15)*, 4803.
29. Che, J.; Jiang, X.; Fan, Y.; Li, M.; Zhang, X.; Gao, D.; Ning, Z.; Li, H. A Novel Dual-Emission Fluorescence Probe Based on CDs and Eu^{3+} Functionalized UiO-66-$(COOH)_2$ Hybrid for Visual Monitoring of Cu^{2+}. *Materials*. **2022**, *15*, 7933.
30. Wang, X. R.; Wang, X. Z.; Du, J.; Huang, Z.; Liu, Y. Y.; Huo, J. Z.; Liu, K.; Ding, B. Post-synthetic dual-emission rhodamine B@ZIF-365 hybrid material and enzymatic biosensor enzyme@ZIF-365: ratiometric temperature sensing, biomolecule nicotinamide detection and sensing platform for lactose and Al^{3+}. *J. Solid State Chem.* **2019,** *279*, 120949.
31. Li, M.; Dong, C.; Yang, J.; Yang, T.; Bai, F.; Ning, Z.; Gao, D.; Bi, J. Solvothermal synthesis of La-based metal-organic frameworks and their color-tunable photoluminescence properties. *Journal of Materials Science: Materials in Electronics.* **2021,** *32, (8)*, 9903-9911.
32. Dong, C.-L.; Li, M.-F.; Yang, T.; Feng, L.; Ai, Y.-W.; Ning, Z.-L.; Liu, M.-J.; Lai, X.; Gao, D.-J. Controllable synthesis of Tb-based metal–organic frameworks as an efficient fluorescent sensor for Cu^{2+} detection. *Rare Metals.* **2021,** *40, (2)*, 505-512.
33. Ashwin, B. C. M. A.; Sivaraman, G.; Stalin, T.; Yuvakkumar, R.; Muthu Mareeswaran, P. Selective and sensitive fluorescent sensor for Pd^{2+} using coumarin 460 for real-time and biological applications. *J. Photochem. Photobiol. B.* **2018,** *183*, 302-308.
34. Feng, L.; Dong, C.; Li, M.; Li, L.; Jiang, X.; Gao, R.; Wang, R.; Zhang, L.; Ning, Z.; Gao, D.; Bi, J. Terbium-based metal-organic frameworks: highly selective and fast respond sensor for styrene detection and construction of molecular logic gate. *J. Hazard. Mater.* **2020,** *388*, 121816.
35. Zhou, Y.; Zhang, D.; Zeng, J.; Gan, N.; Cuan, J. A luminescent lanthanide-free MOF nanohybrid for highly sensitive ratiometric temperature sensing in physiological range. *Talanta.* **2018,** *181*, 410-415.
36. Cadiau, A.; Brites, C. D. S.; Costa, P. M. F. J.; Ferreira, R. A. S.; Rocha, J.; Carlos, L. D. Ratiometric nanothermometer based on an emissive Ln^{3+}-organic framework. *ACS Nano.* **2013,** *7, (8)*, 7213-7218.
37. Fan, X.; Freslon, S.; Daiguebonne, C.; Pollès, L. L.; Calvez, G.; Bernot, K.; Yi, X.; Huang, G.; Guillou, O. A family of lanthanide-based coordination polymers with boronic acid as ligand. *Inorg. Chem.* **2015,** *54, (11)*, 5534-5546.
38. Miyata, K.; Konno, Y.; Nakanishi, T.; Kobayashi, A.; Kato, M.; Fushimi, K.; Hasegawa, Y. Chameleon luminophore for sensing temperatures: control of metal-to-metal and energy back transfer in lanthanide coordination polymers. *Angew. Chem. Int. Ed.* **2013,** *52, (25)*, 6413-6416.
39. Zhao, S.-N.; Li, L.-J.; Song, X.-Z.; Zhu, M.; Hao, Z.-M.; Meng, X.; Wu, L.-L.; Feng, J.; Song, S.-Y.; Wang, C.; Zhang, H.-J. Lanthanide ion codoped emitters for tailoring emission trajectory and temperature sensing. *Adv. Funct. Mater*. **2015,** *25, (9)*, 1463-1469.
40. Meng, X.; Song, S.-Y.; Song, X.-Z.; Zhu, M.; Zhao, S.-N.; Wu, L.-L.; Zhang, H.-J., A Eu/Tb-codoped coordination polymer luminescent thermometer. *Inorg Chem Front.* **2014,** *1, (10)*, 757-760.